

High-frequency and high-temperature electromechanical performances of new PZT–PNN piezoceramics

Franck Levassort^{a,*}, Pascal Tran-Huu-Hue^a, Erling Ringgaard^b, Marc Lethiecq^a

^aLUSSI/GIP Ultrasons, EIVL, François Rabelais University, BP 3410, 41034 Blois cedex, France

^bFerroperm Piezoceramics A/S, Hejreskovvej 18A, DK-3490 Kvistgaard, Denmark

Received 4 September 2000; received in revised form 7 November 2000; accepted 5 December 2000

Abstract

Ferroelectric ceramics based on a solid solution between a PZT ferroelectric phase and a relaxor phase from the lead–nickel–niobium system are characterised. Two different mixed-oxide routes have been used in order to compare the dielectric, piezoelectric and elastic properties of the two ceramics obtained. The characterisation method is based on measurements of the electrical impedance of samples as a function of frequency and allows the determination of the thickness mode resonance parameters. Results are given as a function of frequency (5 to over 25 MHz) and temperature (ambient to over 230°C). Finally, several simulations, using a K.L.M. model, of medical transducers are performed. The results show that the ceramic is well adapted for medical imaging applications, in particular for array transducer configurations. © 2001 Elsevier Science Ltd. All rights reserved.

Keywords: Impedance; Piezoelectric properties; PZT; Transducers

1. Introduction

High quality and high sensitivity ferroelectric materials are required for array or high frequency ultrasonic medical imaging transducers. The main characteristics are a high dielectric constant (over 1500 for the clamped dielectric constant), good temperature (over 100°C) and frequency (over 20 MHz) stability. Moreover, high electromechanical coupling coefficient (thickness coupling coefficient >45%) are needed. The materials characterised in this paper fulfil these requirements. Chemically, they are a solid solution between a conventional PZT phase and a PNN relaxor phase, but the manufacture of these ferroelectric ceramics is based on simple processing routes. Here, two different mixed-oxide routes have been used, i.e. the columbite and the *B*-oxide routes.¹

The goal of this paper is to study and compare the behaviour of these two materials. Therefore, dielectric, mechanical and piezoelectric properties are determined as a function of frequency and temperature.

The next section describes the preparation of the samples with the two processing routes. Then, the characterisation method, based on a fit of the electrical impedance versus frequency of a free resonator in thickness extensional mode on the fundamental and the overtones, is briefly recalled.² This method is applied in the frequency range between 6 and 28 MHz and at temperatures between 20 and 235°C. Finally, these results are used to simulate the performance of an ultrasonic array element for medical imaging applications.

2. Preparation of the samples (Ferroperm Pz21)

The specimens under investigation in this work belong to the PZTNN system, which can be seen as a 3-component system consisting of PbZrO₃, PbTiO₃ and Pb(Ni_{1/3}Nb_{2/3})O₃. Two different mixed-oxide routes have been used, the columbite route and the *B*-oxide route. In the columbite route, NiO and Nb₂O₅ are mixed and calcined to form the columbite-type compound NiNb₂O₆. Subsequently PbO, ZrO₂ and TiO₂ are added and during the second calcination, the PZTNN phase is formed. In the *B*-oxide route, all the oxides going to the *B* site in the *ABO*₃ perovskite structure are

* Corresponding author. Tel.: +33-254-55-84-33; fax: +33-254-55-84-45.

E-mail address: levassort@univ-tours.fr (F. Levassort).

mixed and calcined together. In this case, only PbO remains to be added before the second calcination. The complete fabrication processes is described in Ref. 1.

3. Properties of PZT-PNN disks

The electrical admittance of the thickness mode of a piezoelectric resonator can be expressed by:³

$$Y(\omega) = \left(\frac{i\omega \varepsilon_{33r}^S \varepsilon_0^A}{t} \right) \left[1 - k_t^2 \frac{\tan\left(\frac{\omega t}{2v_l^D}\right)}{\left(\frac{\omega t}{2v_l^D}\right)} \right]^{-1} \quad (1)$$

where ω is the angular frequency (rad s^{-1}), ε_{33r}^S the relative dielectric constant at constant strain (i.e. clamped), ε_0 the dielectric constant of vacuum (F m^{-1}), A the electrode area (m^2), t the thickness (m), k_t the electromechanical coupling factor in thickness mode, v_l^D the longitudinal wave velocity (m s^{-1}), ρ the density (kg m^{-3}), C_{33}^D the elastic stiffness coefficient at constant electrical displacement (N m^{-2}) and e_{33} the piezoelectric coefficient (C m^{-2}).

Mechanical (δ_m) and dielectric (δ_e) losses are introduced,⁴ thus complex elastic coefficient (C_{33}^{E*}) and relative dielectric constant (ε_{33r}^{S*}) are used in Eq. (1):

$$C_{33}^{E*} = C_{33}^E (1 + i\delta_m) \quad \varepsilon_{33r}^{S*} = \varepsilon_{33r}^S (1 - i\delta_e) \quad (2)$$

Using the geometrical characteristics (electrode area and thickness) and the density of the different samples, a fit of the experimental electrical impedance with Eq. (1) allows the determination of all other parameters. For the materials studied here, these parameters show a low variation versus frequency when observed around a particular resonant frequency, so they can be assumed constant in the range of the fit.

The experimental set-up is composed of a HP4195 impedance analyser and its impedance test kit with a spring clip-fixture where the ceramic disks are placed under free piezoelectric resonator conditions.

3.1. Frequency characterisation

The method described above is applied to the fundamental resonance as well as to the overtones. Then, precise values of the parameters are deduced at the considered frequency. Table 1 gives the dimensions and the results for the ceramic disks obtained respectively by the columbite and *B*-oxide routes, measured in the frequency range corresponding to the third overtones (6.5 MHz).

Measurements have been performed on five different overtones (between the 3rd and 13th overtones). Using these fits, the behaviour of all parameters can be extracted as a function of frequency (between 6 and 28 MHz). Fig. 1 shows the frequency dependence of the thickness mode coupling factor. For the columbite route, the variation observed ($-6.2 \times 10^{-3} \text{ MHz}^{-1}$ with a linear regression in the studied frequency range) is slightly higher, but in the same order of magnitude as those obtained in.^{2,5,6} For the *B*-oxide route, the variation is higher ($-16 \times 10^{-3} \text{ MHz}^{-1}$).

The elastic constants (C_{33}^D) are represented in Fig. 2. The sample made by the *B*-oxide route has higher values as well as higher frequency dependence. The relative dielectric constants ε_{33r}^S are around 1760 for both ceramics (Table 1). The piezoelectric coefficients (e_{33}) can also be deduced. They decrease when frequency increases (for both materials), which explains the decrease of the thickness coupling factor (k_t) as shown in Fig. 1. Mechanical and dielectric losses are shown in Fig. 3. The frequency dependence for the two PZT-PNN ceramics is nearly linear. The low frequency losses are similar for both ceramics, but the *B*-oxide route material shows slightly higher frequency variations than the columbite sample.

Table 1
Electromechanical properties of Pz21 ceramics made by two mixed-oxide routes (i.e. columbite and *B*-oxide) measured at the 3rd overtone (6.5 MHz)

Pz21 ceramic	A^a (mm^2)	ρ^b (kg m^{-3})	f_a^c (MHz)	v_l^d (m s^{-1})	k_t^e (%)	$\varepsilon_{33}^S/\varepsilon_0^f$	δ_e^g (%)	δ_m^h (%)
Columbite	190	7825	2.16	4495	48.5	1750	2.6	0.9
<i>B</i> -oxide	193	7800	2.11	4450	48.2	1775	2.5	1.1

^a A , Electrode area.

^b ρ , Density.

^c f_a , Antiresonance frequency.

^d v_l , Longitudinal velocity.

^e k_t , Thickness mode coupling factor.

^f $\varepsilon_{33}^S/\varepsilon_0$, Relative dielectric constant at constant strain.

^g δ_e , Dielectric losses.

^h δ_m , Mechanical losses.

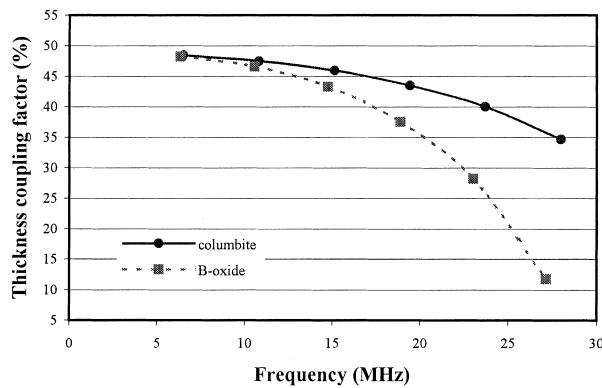


Fig. 1. Thickness mode coupling factor (k_t) as a function of frequency for Pz21 ceramics made by two mixed-oxide routes (i.e. columbite and B -oxide) measured at the 3rd overtone.

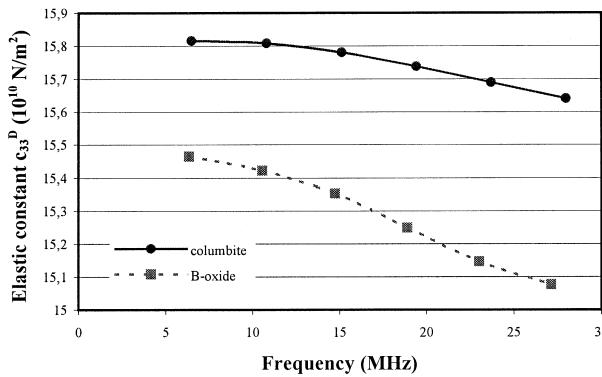


Fig. 2. Elastic constant (c_{33}^D) as a function of frequency for Pz21 ceramics made by two mixed-oxide routes (i.e. columbite and B -oxide) measured at the 3rd overtone.

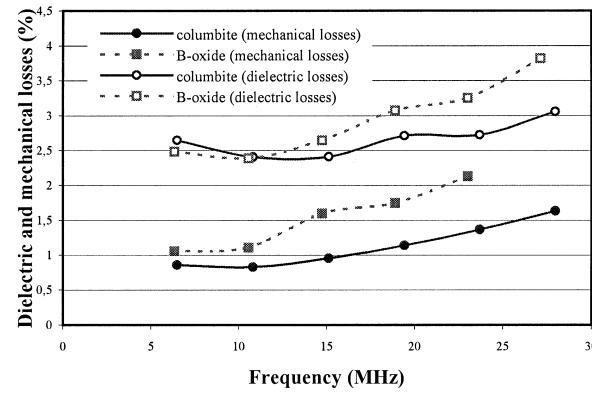


Fig. 3. Mechanical (δ_m) and dielectric (δ_e) losses as a function of frequency for Pz21 ceramics made by two mixed-oxide routes (i.e. columbite and B -oxide) measured at the 3rd overtone.

3.2. Temperature characterisation

Measurements at elevated temperatures were performed by heating poled ceramic disks in a temperature controlled chamber between 20 and 235°C. The heating rate was 2°C min⁻¹. A specific test fixture was designed

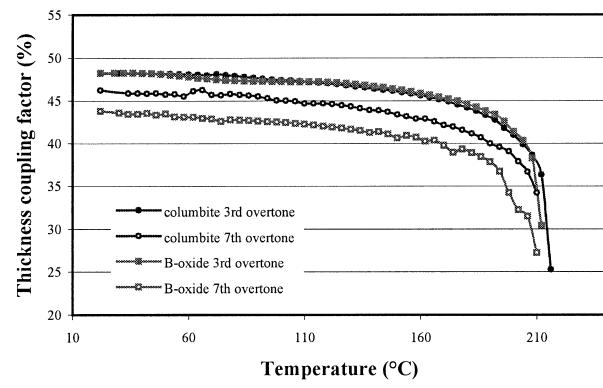


Fig. 4. Thickness mode coupling coefficient (k_t) as a function of temperature for Pz21 ceramics made by two mixed-oxide routes (i.e. columbite and B -oxide) measured at both the 3rd and 7th overtones.

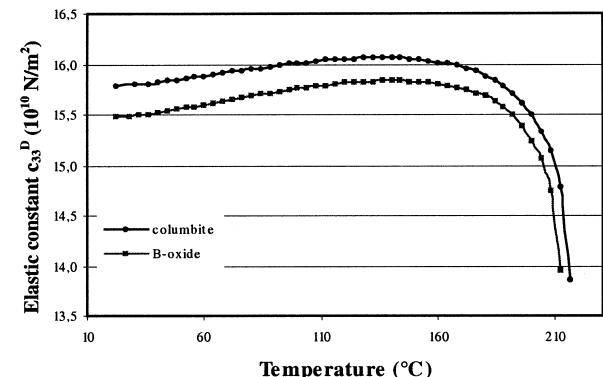


Fig. 5. Elastic constant (c_{33}^D) as a function of temperature for Pz21 ceramics made by two mixed-oxide routes (i.e. columbite and B -oxide) measured at the 3rd overtone.

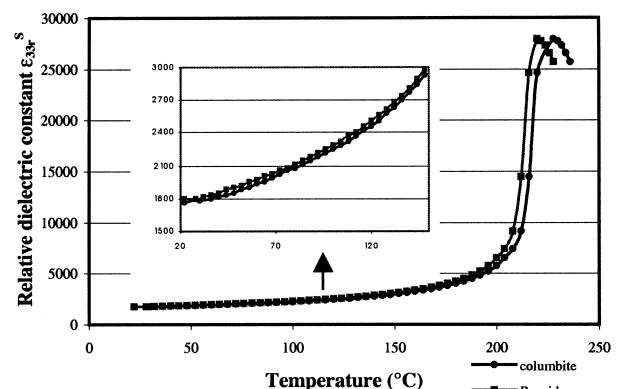


Fig. 6. Dielectric constant at constant strain ($\epsilon_{33}^S/\epsilon_0$) as a function of temperature for Pz21 ceramics made by two mixed-oxide routes (i.e. columbite and B -oxide) measured at the 3rd overtone.

for these conditions. The measurements were performed on the 3rd (6.5 MHz) and 7th (15 MHz) overtones with 4°C steps for two samples.

Fig. 4 represents the temperature dependence of the thickness coupling factor (k_t) for the two samples (3rd and 7th overtones). Between 20 and 160°C, the

Table 2

Properties of Pz21 ceramics made by two mixed-oxide routes (i.e. columbite and *B*-oxide) measured at the 7th overtone (15 MHz) and used for array-transducer element simulation

Pz21 ceramics	v_1^a (m s $^{-1}$)	k_t^b (%)	$\varepsilon_{33}^S/\varepsilon_0^c$	δ_m^d (%)	δ_e^e (%)	e_{33}^f (C m $^{-2}$)
<i>B</i> -oxide (20°C)	4440	43.8	1755	1.4	3.6	21.4
<i>B</i> -oxide (150°C)	4480	40.6	3005	1.2	7.5	22.6
Columbite (20°C)	4495	46.2	1725	1.0	2.0	22.6
Columbite (150°C)	4530	43.4	2900	0.8	4.4	27.8

^a v_1 , Longitudinal velocity.

^b k_t , Thickness mode coupling factor.

^c $\varepsilon_{33}^S/\varepsilon_0$, Relative dielectric constant at constant strain.

^d δ_m , Mechanical losses.

^e δ_e , Dielectric losses.

^f e_{33} , Piezoelectric coefficient.

variation for the columbite and *B*-oxide routes are respectively -1.9×10^{-4} °C $^{-1}$ and -1.5×10^{-4} °C $^{-1}$. These values are very low, and shows that the *B*-oxide route in particular allows to achieve very high temperature stability.

For the calculation of the elastic, dielectric and piezoelectric constants, the thickness and density are assumed to be constant (i.e. dilatation can be neglected).

Elastic constants (C_{33}^D) are shown in Fig. 5. These stiffnesses increase slightly between room temperature and around 140°C and then quickly decrease. Fig. 6 represents the relative dielectric constant at constant strain ($\varepsilon_{33}^S/\varepsilon_0$). The two routes yield approximately the same values. The Curie–Weiss temperature, determined by the maximum of permittivity, is found at 224 °C for the *B*-oxide route and 232°C for the columbite route. Between 20 and 160°C the relative variation is 0.31% °C $^{-1}$ for the two samples. Comparable soft PZT materials typically have temperature coefficients¹ of 0.5% °C $^{-1}$.

The piezoelectric coefficients (e_{33}) increase between 20 and 210°C (relative variation of 40%) for the two samples (several values are given in Table 2).

The increase of ($\varepsilon_{33}^S/\varepsilon_0$) is compensated by the increase of (e_{33}) to obtain a very good stability for the thickness coupling factor (k_t).

4. Transducer simulations

With an equivalent electrical circuit model (K.L.M.),⁷ two simulations of an array element have been performed integrating the sample made by the *B*-oxide route, considering two different operating temperatures (20 and 150°C).

The specifications of the transducer are the following:

- Dimensions: 150 μm × 4.5 mm.
- Matching layer: acoustical impedance ($Z_1 = 3.4$ MRa), longitudinal wave velocity ($v_1 = 2650$ m s $^{-1}$) and thickness ($e_1 = 44$ μm).

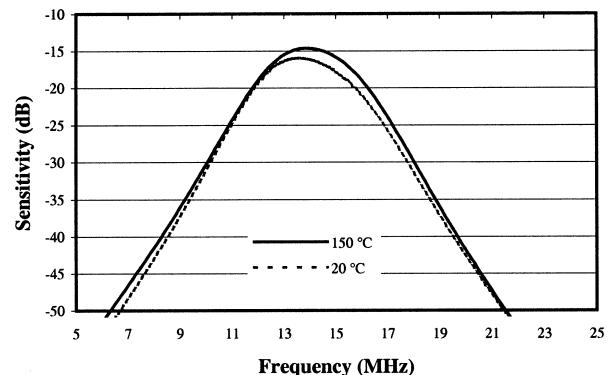


Fig. 7. 50 Ω loop sensitivity for an array-transducer element (15 MHz) operating at ambient temperature and at 150°C.

- Backing: acoustical impedance ($Z_b = 6$ MRa). This element is considered as having at semi-infinite thickness.
- Resonant frequency of the piezoelectric element: $f = 15$ MHz. This frequency corresponds to the 7th overtone. The values used for the simulation concerning the piezoelectric element are those given in Table 2. Between the two simulations, the properties of the backing and matching layer are assumed constant: only the properties of the piezoelectric element change according to measurements described in Section 3.2.

The 50 Ω loop sensitivities, represented in Fig. 7, show that the overall properties of the transducer are very stable with temperature. The sensitivities at the centre frequency are -16 and -14.6 dB for 20 and 150°C, respectively. The -6 dB bandwidths are 35 and 34%, respectively, for the same temperatures as above.

5. Conclusion

A composition based on a ternary PZT/relaxor system has been studied. Characterisations have been made

as a function of temperature and frequency. The results for two mixed oxide routes (columbite and *B*-oxide) are similar for the temperature variations. These ceramics show a high stability of the electromechanical thickness coupling factor and the dielectric constant from room temperature to over 150°C. These properties are used as inputs for simulations of transducers for medical imaging applications. The transducer shows high sensitivity (due to high coupling factor and dielectric constant) and relatively large bandwidth even at elevated temperatures.

Concerning their behaviour as a function of frequency, the columbite route is slightly more stable than the *B*-oxide route. A study of the microstructure will be necessary to give a complete interpretation of these experimental results.

Acknowledgements

This work was funded by the French Research Ministry in the on-going EUREKA project PIMET (EU1664).

References

1. Bove, T., Wolny, W., Ringgaard, E. and Pedersen, A., New piezoceramic PZT-PNN material for medical diagnostics applications. *J. Eur. Ceram. Soc.*, 2001, this issue.
2. Tran-Huu-Hue, L. P., Levassort, F., Felix, N., Damjanovic, D., Wolny, W. and Lethiecq, M., Comparison of several methods to characterise the high frequency behaviour of piezoelectric ceramics for transducer applications. *Ultrasonics*, 2000, **38**, 219–223.
3. IEEE Standard on Piezoelectricity ANSI/IEEE Std., IEEE, New York, 1987.
4. Lethiecq, M., Tran Huu Hue, L. P., Patat, P. and Pourcelot, L., Measurement of losses in five piezoelectric ceramics between 2 and 50 MHz. *IEEE Trans. Ultrason. Ferro. Freq. Control*, 1993, **40**(3), 232–237.
5. Foster, F. S., Ryan, L. K. and Turnbull, D. H., Characterization of lead zirconate titanate ceramics for use in miniature high-frequency (20–80 MHz) transducers. *IEEE Trans. Ultrason. Ferro. Freq. Control*, 1991, **38**(5), 446–453.
6. Zipparo, M. J., Shung, K. K. and Shrout, T. R., Piezoceramics for high-frequency (20 to 100 MHz) single-element imaging transducers. *IEEE Trans. Ultrason. Ferro. Freq. Control*, 1997, **44**(5), 1038–1048.
7. Krimholz, R., Leedom, D. A. and Mathei, G. L., New equivalent circuit for elementary piezoelectric transducers. *Electron. Lett.*, 1970, **38**, 398–399.